

SUPPLEMENTARY DATA

Filaggrin 2 deficiency results in abnormal cell-cell adhesion in the cornified cell layers and causes peeling skin syndrome type A

Janan Mohamad^{1,2}, Ofer Sarig¹, Lisa M. Godsel³, Alon Peled^{1,2}, Natalia Malchin¹, Ron Bochner¹, Dan Vodo^{1,2}, Tom Rabinowitz⁴, Mor Pavlovsky¹, Shahar Taiber^{1,2}, Maya Fried^{1,2}, Marina Eskin-Schwartz^{1,2}, Siwar Assi⁵, Noam Shomron^{4,6}, Jouni Uitto⁷, Jennifer L. Koetsier³, Reuven Bergman^{8,9}, Kathleen J. Green^{3,10}, Eli Sprecher^{1,2}

¹Department of Dermatology, Tel Aviv Sourasky Medical Center, Tel Aviv, Israel;

²Department of Human Molecular Genetics & Biochemistry, Sackler Faculty of Medicine, Tel Aviv University, Tel Aviv, Israel; ³Department of Pathology, Northwestern University

Feinberg School of Medicine, Chicago, Illinois, USA; ⁴Department of Cell and Developmental Biology, Sackler Faculty of Medicine, Tel Aviv University, Tel Aviv, Israel;

⁵Research Center for Digestive Disease, Sourasky Medical Center and Sackler Faculty of

Medicine, Tel-Aviv, Israel; ⁶Variantyx, Ltd, Framingham, USA; ⁷Department of Dermatology and Cutaneous Biology, Sidney Kimmel Medical College at Thomas Jefferson University,

Philadelphia, Pennsylvania, USA; ⁸Department of Dermatology, Rambam Health Care

Campus, Haifa, Israel; ⁹Rappaport Faculty of Medicine, Technion–Israel Institute of

Technology, Haifa, Israel; ¹⁰Department of Dermatology, Northwestern University Feinberg School of Medicine, Chicago, Illinois, USA

SUPPLEMENTARY MATERIAL and METHODS

Exome sequencing

Exome sequencing was performed by Otogenetics Ltd. Whole-exome capture was carried out by in-solution hybridization with SureSelect Human All Exon Version 5.0 (Agilent, Santa Clara, USA) followed by massively parallel sequencing (Illumina HiSeq2500) with 125-bp paired-end reads. Reads were aligned to the Genome Reference Consortium Human Build 37 (GRCh37/hg19) using Burrows-Wheeler (Li and Durbin, 2010). Duplicate reads, resulting from PCR clonality or optical duplicates, and reads mapping to multiple locations were excluded from downstream analysis. Reads mapping to a region of known or detected insertions or deletions were re-aligned to minimize alignment errors. Single-nucleotide substitutions and small insertion deletions were identified and quality filtered using the Genome Analysis Tool Kit (GATK) (McKenna et al., 2010). Rare variants were identified by ANNOVAR (Wang et al., 2010) and filtered using data from dbSNP142, the 1000 Genomes Project, HGMD, gnomAD, Ensemble, Exome Variant Server, and an in-house database of individual exomes. Variants were classified by predicted protein effects using Polyphen2 (Adzhubei et al., 2010) and SIFT (Kumar et al., 2009). Validation and co-segregation of the disease phenotype with the mutation were verified using Sanger sequencing. Table S1 summarizes exome sequencing details.

Mutation analysis

Genomic DNA was PCR-amplified using oligonucleotide primer pairs spanning the entire coding sequence as well as intron–exon boundaries of *CDSN*, *CSTA*, *CHST8* and *FLG2* (Table S2) with Taq polymerase (Qiagen, Hilden, Germany) or Takara LA Taq (Takara Bio Inc, Kusatsu, Japan). Cycling conditions in the case of the *CDSN*, *CSTA*, *CHST8* genes were as follows: 94°C, 2 min; 94°C, 40 sec; 61°C, 40 sec; 72°C 50 sec, for 3 cycles, 94°C, 40 sec; 59°C, 40 sec; 72°C 50 sec, for 3 cycles, 94°C, 40 sec; 57°C, 40 sec; 72°C 50 sec, for 34 cycles. To amplify exon 2 and 3 of *FLG2*, cycling conditions were as followed: 94°C, 2 min; 94°C, 40 sec; 61°C, 40 sec; 72°C 30 sec, for 3 cycles, 94°C, 40 sec; 59°C, 40 sec; 72°C 30 sec, for 3 cycles, 94°C, 40 sec; 57°C, 40 sec; 72°C 30 sec, for 34 cycles.

Gel-purified (QIAquick gel extraction kit, QIAGEN, Hilden, Germany) amplicons were subjected to bidirectional DNA sequencing with the BigDye terminator system on an ABI Prism 3100 sequencer (Applied Biosystems, Foster City, NY, USA) using either oligonucleotides used for PCR amplification or additional primers (Table S3).

PCR-restriction fragment length polymorphism (RFLP)

To screen for the c.1065T>A mutation, we PCR-amplified a 185 bp fragment with Taq polymerase (Qiagen, Hilden, Germany) and the following oligonucleotides 5`-TGAGTCTA ACCCCTGTAGTCAGTCCTATAGTCAGAGAGGT -3` and 5`-GGCCACAGGAACCAT ATTCA -3`. PCR cycling conditions were as follows: 94°C, 2 min; 94°C, 40 sec; 61°C, 40 sec; 72°C 30 sec, for 3 cycles; 94°C, 40 sec; 59°C, 40 sec; 72°C 30 sec, for 3 cycles; 94°C, 40 sec; 57°C, 40 sec; 72°C 30 sec, for 34 cycles. PCR products were then incubated at 37°C for 16 hours with MseI (New

England Biolabs, Frankfurt, Germany) followed by 20 min of inactivation at 65°C. The digested PCR products were electrophoresed in ethidium bromide-stained 3% agarose gels.

Quantitative RT-PCR

For quantitative real-time PCR (qRT-PCR), cDNA was synthesized from 1000 ng of total RNA using qScript kit (Quanta Biosciences, Gaithersburg, MD, USA). cDNA PCR amplification was carried out with the PerfeCTa SYBR Green FastMix (Quanta Biosciences, Gaithersburg, MD, USA) on a StepOnePlus system (Applied Biosystems, Waltham, MA, USA) with gene-specific intron-crossing oligonucleotides (Table S4). Cycling conditions were as follows: 95°C, 20 sec and then 95°C, 3 sec; 60°C, 30 sec for 40 cycles. Each sample was analyzed in triplicates. For each set of primers, standard curves were obtained with serially diluted cDNAs. Results were normalized to *GAPDH* mRNA levels.

Immunohistochemistry and immunofluorescence studies

The following primary antibodies were used: polyclonal rabbit anti human filaggrin2 (diluted 1:200; Leica Biosystems, Newcastle upon Tyne, UK), monoclonal mouse anti human filaggrin (diluted 1:40; Leica Biosystems, Newcastle upon Tyne, UK); polyclonal sheep anti human CDSN (diluted 1:500; Thermo Fisher Scientific, Waltham, MA , USA); monoclonal rabbit anti human KRT10 (diluted 1:50; Abcam, Cambridge, MA, USA); monoclonal mouse anti KRT14 (diluted 1:50; Abnova, Walnut, CA, USA); polyclonal rabbit anti-loricrin (diluted 1:200; Abcam, Cambridge,

MA, USA); mouse anti E-Cadherin (diluted 1:600, Invitrogen, Carlsbad, CA, USA); monoclonal mouse anti human Dsg1 (straight supernatant; P124; Progen Biotechnik, Heidelberg, Germany); monoclonal mouse anti-human Dsc1 (1:50, U100; Progen Biotechnik) and rabbit anti-keratin 5 and keratin 10 (1:500; gifts from J. Segre, National Human Genome Research Institute). The specificity of the filaggrin-2 antibody was confirmed using filaggrin family member 2 recombinant protein Antigen (Novus Biologicals, Littleton, CO, USA) which was mixed with the primary antibody (diluted, 1:200 with the antigen diluted to 100 molar excess) and incubated overnight at 4°C prior to staining (Figure S9). Negative controls consisted of slides processed similarly while omitting the primary antibody.

For immunohistochemistry, following antigen retrieval with 0.01M citrate buffer, pH 6.0 (Invitrogen, Carlsbad, CA) in a microwave for 25 min and blocking with hydrogen peroxide for 10 min and protein block for 40 min, 5 µm-thick paraffin-embedded sections on ®Plus glass slides (MenzelGlazer, Braunschweig, Germany) were processed using an automated immunostainer (Benchmark-XT, Ventana Medical System, Tucson, AZ, USA). Visualization of the bound primary antibodies was performed using the I-View DAB detection kit (Ventana Medical System). The sections were then counterstained with Gill's hematoxylin, dehydrated and mounted for microscopic examination.

For immunofluorescence analysis of skin biopsies, the procedure was similar except for blocking with 2% bovine serum albumin (BSA) in phosphate-buffered saline (PBS) for 30 min at room temperature. Coverslips were mounted in DAPI Fluoromount-G (Southern Biotechnologies, Birmingham, AL, USA). Specimens were examined using a Nikon 50I microscope connected to DS-R11 digital camera or AxioVision Z1 epifluorescence microscope (Carl Zeiss) fitted with an Apotome 2

slide module, AxioCam MRm digital camera and a 40x objective (Plan-Neofluar, NA 0.5, Carl Zeiss) and a maximum image projection was compiled. Fluorescence signal was quantified using the NIS-Elements BR 3.6 software. Seven measurements were performed per field for each fluorescence staining and normalized to the field area. Two sided t-test was used to assess statistical significances. For cell immunofluorescence studies, primary keratinocytes were grown on glass coverslips and fixed with 4% paraformaldehyde. Following permeabilization with 0.1% Triton/PBS, Sections were blocked in 2% BSA. Primary antibodies were diluted in 2% BSA and incubated overnight at 4 °C. Primary antibodies used were polyclonal rabbit anti filaggrin2 (diluted 1:400; Leica Biosystems, Newcastle upon Tyne, UK), polyclonal sheep anti human CDSN (diluted 1:200; Thermo Fisher Scientific, Waltham, MA , USA); monoclonal mouse anti DSG1 (ready to use, PROGEN Biotechnik GmbH, Heidelberg, Germany), mouse anti E-Cadherin (diluted 1:400, Invitrogen, Carlsbad, CA, USA). Secondary antibody staining was carried out for 1 hour at 37 °C using Rhodamine RED X or Alexa flour 488 anti-mouse , anti-rabbit or anti sheep secondary antibodies (Life Technologies/Invitrogen). Coverslips were mounted in polyvinyl alcohol. Imaging was done with an LSM 510 confocal microscope (Zeiss, Germany). Postacquisition processing of confocal stacks (3D imaging) was performed using Deconvolution– Huygens software.

Organotypic cell cultures

Patient and control models generation was modified from a previously published protocol (Mildner et al., 2006), using $0.1 \cdot 10^6$ fibroblasts per ml of type I Bovine Collagen matrix (Advanced BioMatrix; PureCol®; San Diego, CA, USA) and $1.0 \cdot 10^6$ keratinocytes per cm^2 growth area in a 3- μm filter tissue culture insert (BD, Franklin

Lakes, NJ, USA). Forty eight hours after harvesting, control and patient fibroblasts were trypsinized, counted and resuspended in DMEM medium containing 20% Fetal Calf Serum (Biological Industries). Bovine Collagen I, fibroblasts, and serum were mixed and 2.5 ml of this solution was poured into each filter insert and allowed to gel for 2 hours at 37°C in a humidified atmosphere. The gels were then equilibrated with KGM (Walkersville, MD, USA) for 2 hours. Keratinocytes were seeded onto the matrix in a total volume of 2 ml medium per insert. After 24 hours, the system was raised to air-liquid interface and medium was changed to Keratinocyte Culture Medium (KCM) as previously described (Fuchs-Telem et al., 2011). The organotypic cell cultures were maintained at 37°C for 8 days and then grown for another 2 days either at 37°C or 40°C. Medium was changed every second day. For each set of experiments, keratinocytes and fibroblasts were derived from the same donor and used at the third passage. Punch biopsies were obtained from organotypic cell cultures and fixed in 4% paraformaldehyde. Five µm-thick paraffin-embedded sections were processed for hematoxylin eosin staining.

Western blotting

Cells were homogenized in Cellytic MT lysis/extraction reagent (Sigma-Aldrich) and a protease inhibitor mix, including 1 mM phenylmethanesulphonylfluoride, and 1 mg ml⁻¹ aprotinin and leupeptin (Sigma-Aldrich). Following centrifugation at 10,000 × g for 10 minutes at 4 °C, proteins were electrophoresed through a 7.5% SDS-PAGE and transferred onto a nitrocellulose membrane (Trans-Blot, Bio-Rad, Hercules, CA). After blocking for 1 hour using 1 × TBST (50 mM Tris, 150 mM NaCl, 0.01% Tween 20) with 3% BSA, blots were incubated over-night at 4 °C with primary monoclonal mouse anti human corneodesmosin (diluted 1:500;

Abnova, Walnut, CA, USA) or with rabbit anti-human Fillagrin 2 (diluted 1:1000; Novus Biologicals). The blots were washed 5 times 5 min each with 1 × TBST with 1.5% BSA. After incubation with secondary horseradish peroxidase-conjugated anti-rabbit Ab (diluted 1:5000; Sigma-Aldrich) or horseradish peroxidase-conjugated goat anti-mouse Ab (diluted 1:10,000; Jackson ImmunoResearch laboratories, PA, USA), and subsequent washings (5 times 5 min each with 1 × TBST), proteins were detected using the EZ-ECL chemiluminescence detection kit (Biological Industries). To compare the amount of protein in different samples, the blots were re-probed using a mouse mAb to β -actin (Sigma-Aldrich). Protein levels were quantified by ImageJ software.

SUPPLEMENTARY TABLES

Table S1

Exome sequencing

	II-8	I-3
Average read depth	110	134
% of exome >1x	99.7	99.8
% of exome >8x	99.1	99.3
% of exome >20x	97.8	98.3

Table S2**Oligonucleotides used for gDNA amplification**

Gene	Exon (number_part)	Forward oligonucleotide sequence	Reverse oligonucleotide sequence	Expected product size (bp)
<i>CDSN</i> (<i>Oji et al,</i> <i>2010</i>)	1	CTCTCCCCACAGTGACTCCT	AAACTTACCTGAGGCGACCA	300
	1_1	TGGGAGAAACCCGAGAGG	GCTGCTGAACTGAAAGCTG	515
	1_2	GAAGCAGCAGCTCTCATTCG	CTTACTGTAGGTCATGCCTGGAA	505
	1_3	TGGGTGGCTCCTCTGACA	CACAAGGCTGAAGGATGATTT	453
	1_4	CAGCAGCTCCAGTCCCAAT	GGCACTGGACTTCTCCATA	377
<i>CSTA</i> (<i>Blaydon</i> <i>et al,</i> <i>2011</i>)	1	AAGCAAGAAGACTTGCCTGG	GTCACACTCACAGTTTGGGG	438
	2	TTTTAGGAGGATGAGGTTCCC	CCGTAAGGAAGGAATTATGTGG	290
	3	TAGCAATGCTGTTCCTCAGC	TCCAATTGCCATCAATTTATATG	469
	EST (BE181757)	AAAAAGTCAGGGTGCCAAAA	AGAGCTCGAATGGAGGTCAAG	571
<i>CHST8</i> (<i>Cabral et</i> <i>al, 2012</i>)	2	TCGGTGATGACTATCCCTCC	CAAGCCCAGCACACCAG	339
	3	CCTTCCCTAGAGCCTACCC	GGGAAAGGCTGGACACATT	291
	4_1	CACCTGAGAGGGACAGGAAC	TGGGCACCTCGCAGTAG	535
	4_2	GAGGCCTGCGCCAAGTA	GGTCCCAGTGAATGTCCATC	505
	4_3	TACTATCACCCGGTCTTCGG	CTGTTGCTCCCAGGATGAG	540
<i>FLG2</i>	2	AATGAAAATTGCTGATAAAAGG	TGCTTAGAGTTACTGGGGC	328
	3	ATGGCTGTGTCTCAGGAGGT	GGCCACAGGAACCATATTCA	228
	3_1	AAATGTGTTAGTTGAGTATGCAGG	ATACTCCTCCCAGATTCCC	597
	3_2	TGGTCATTCATGGAGTGGTG	GAGCCTGTTCTCCATTGTCC	564
	3_3	CTTGCTTCTGCGAACTGTGG	GGGACTGGTTCAGGACAATC	770
	3_4	TGGAGAACAGGCTCAAGTCA	TGTTGAGATTCACCCTGGCC	2567
	3_5	TCAGTCCACTGGATTGGCC	AAGCAGAAGGAACCAGAGCC	4457

Table S3**Additional oligonucleotides used for *FLG2* gDNA sequencing**

Exon (number_part)	Oligonucleotide sequence
3_4	TTGACCTGAGCCCAACCC
3_4	TCAAGTTCAGGACAGACATC
3_4	ATCTAGACTCATATTGTCC
3_4	CCTGTGTTGTCCAAATCCAAAAGTCTGTCCTG
3_4	CAGGACAGACTTTTGGATTTGGACAACACAGG
3_5	AGACCTGGCTTGGCTGTGTG
3_5	ATGCCCACTATCATCATGGATTA
3_5	AAAGACAGCCAGGATCCAC
3_5	ACTGAAAATGACTTGCTCTAC
3_5	ATATCCAGGTTGAACATAGG

Table S4

Oligonucleotides used for qPCR

Gene	Forward oligonucleotide sequence	Reverse oligonucleotide sequence	Expected size (bp)
<i>GAPDH</i>	GAGTCAACGGATTGGTCGT	GACAAGCTTCCCGTTCTCAGCC	185
<i>FLG2</i>	TGAAGAACCCAGATGATCCA	CATCAAAAGAAACTCAGTAAAGTCC	97

Table S5

Donor of control skin biopsies

Control #	Age	Sex	Biopsy site
1	33	Male	Abdomen
2	29	Female	Left thigh
3	65	Male	Left flank

SUPPLEMENTARY FIGURES

Figure S1



Figure S1. Extensive skin peeling and crusting in individual II-8 at age 8 years.

The phenotype of the patient was more severe at young age than seen in adulthood.

Figure S2

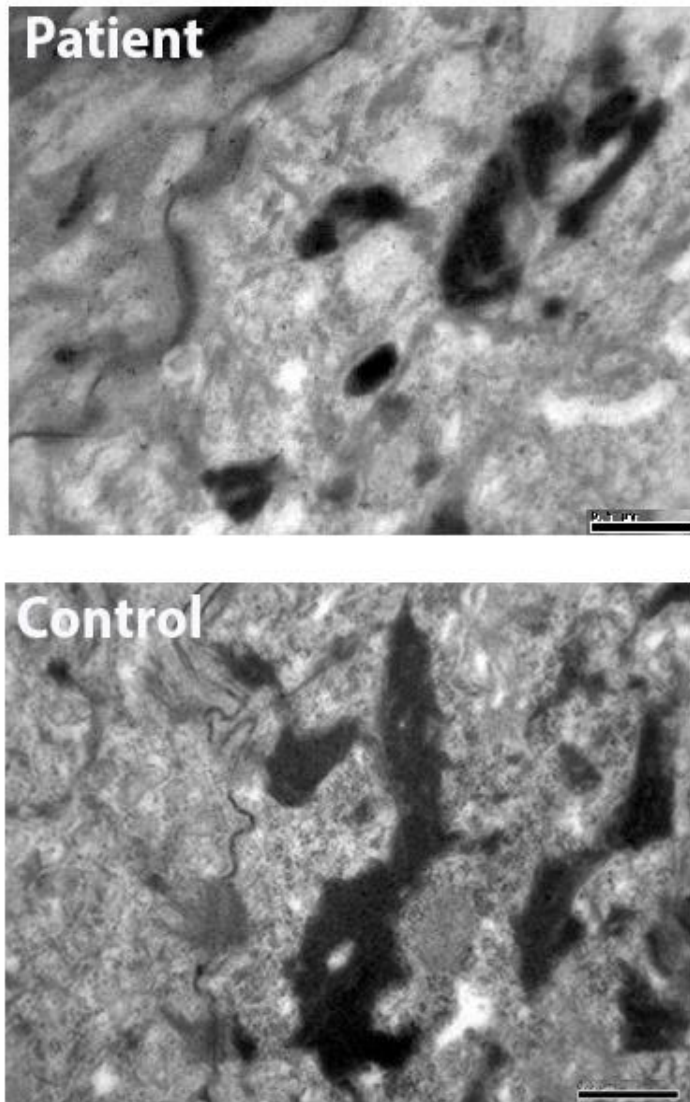


Figure S2. Electron microscopy of the granular layer. Deformed and irregularly shaped keratohyaline granules are seen in patient keratinocyte cytoplasm at a distance from desmosomes. In contrast, keratohyaline granules from a healthy age-matched control individual demonstrate a stellate and angulated shape, and localize next to the desmosomes (scale bar = 0.5 μm).

Figure S3

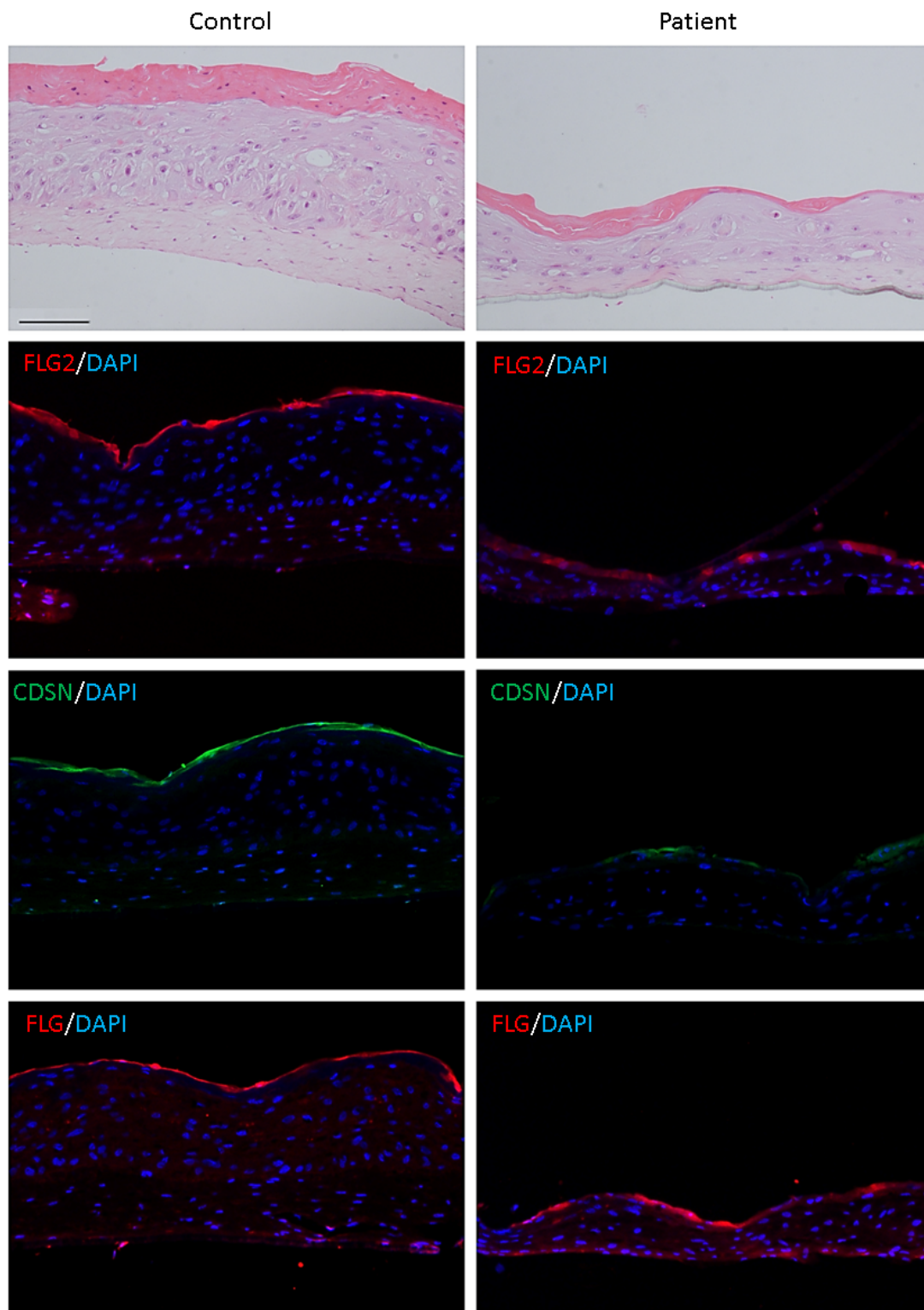


Figure S3. Organotypic cell cultures. Primary keratinocytes and fibroblasts cell cultures were established from a healthy individual (Control) or from patients II-8 (Patient) and were used to generate skin equivalents. Punch biopsies were obtained from skin equivalents at day 10 and stained for hematoxylin and eosin (upper panel) or for various epidermal proteins (lower panels) including filaggrin 2 (FLG2), corneodesmosin (CDSN) and filaggrin (FLG) (scale bar =100 μ m).

Figure S4

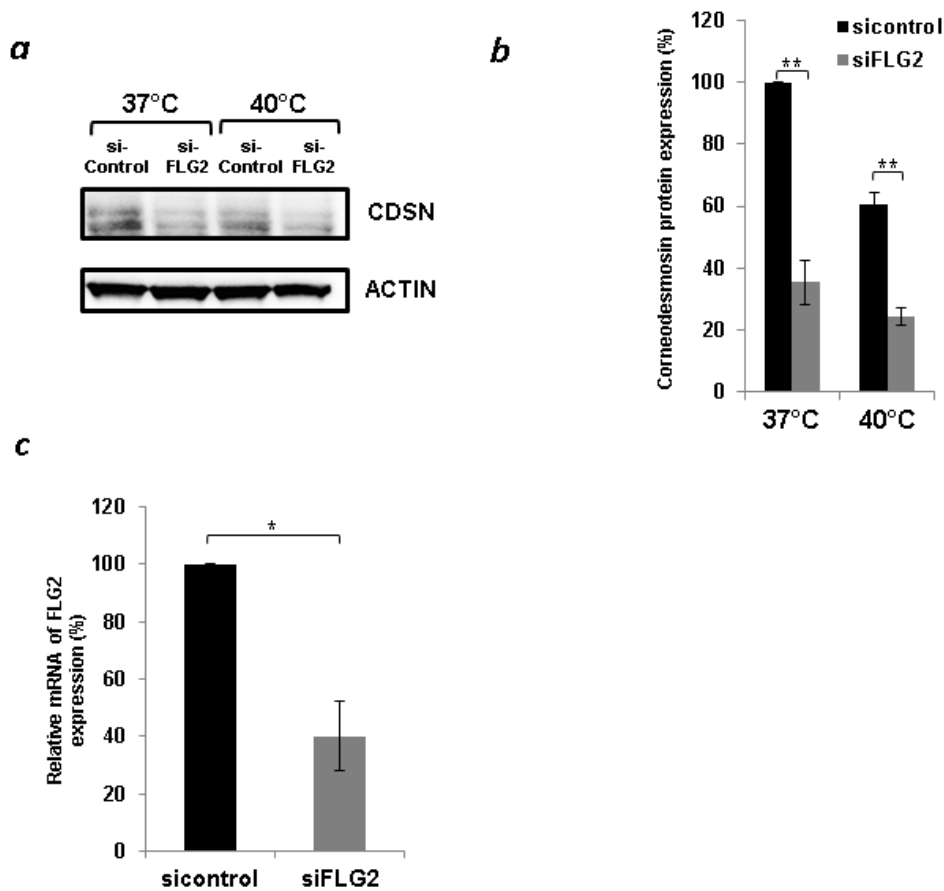


Figure S4. Corneodesmosin protein expression in keratinocytes down-regulated for *FLG2*. (a) Corneodesmosin protein expression in human primary keratinocytes grown at two different temperatures (37°C and 40°C) transfected with control siRNA or *FLG2*-specific siRNA was ascertained using immunoblotting with anti corneodesmosin antibody (β -actin served as a loading control); (b) Protein levels were quantified by ImageJ software and normalized to levels observed in siControl transfected keratinocytes at 37°C; (c) *FLG2* mRNA levels were quantified using qRT-PCR. Analysis was performed in parallel to the Western blot. Results were normalized to *GAPDH*, represent the mean of two experiments and are expressed as percentage of RNA expression relative to expression in control samples \pm SEM (two sided t-test: * $p < 0.05$).

Figure S5

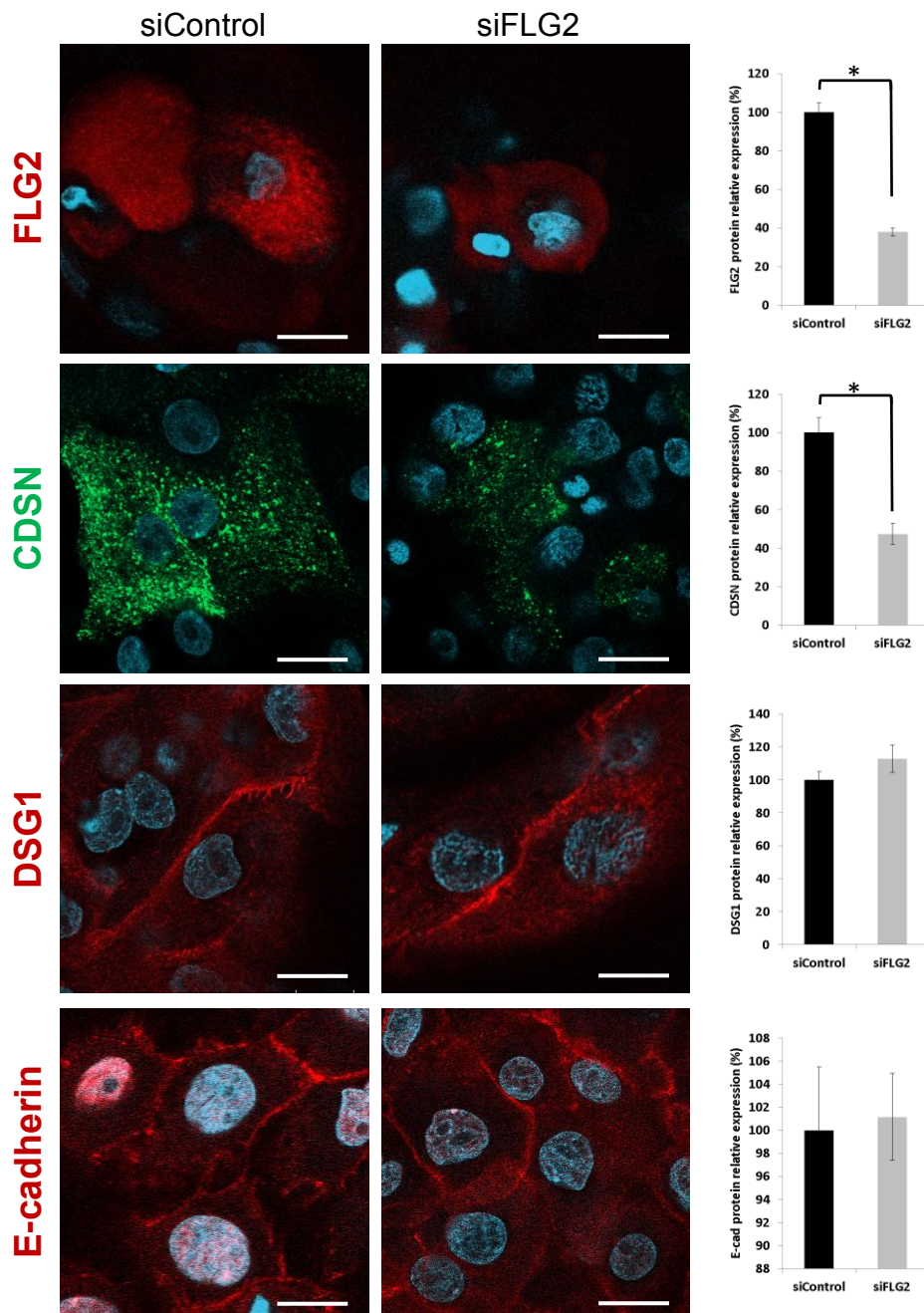


Figure S5. Protein expression in keratinocytes after *FLG2* silencing. Different proteins expression in human primary keratinocytes transfected with control siRNA or *FLG2* siRNA was ascertained using immunofluorescence staining. Immunofluorescence staining intensity was quantified (see graphs at the right of the images), (two sided t-test: * $p < 0.05$) (scale bar = 20 μm).

Figure S6

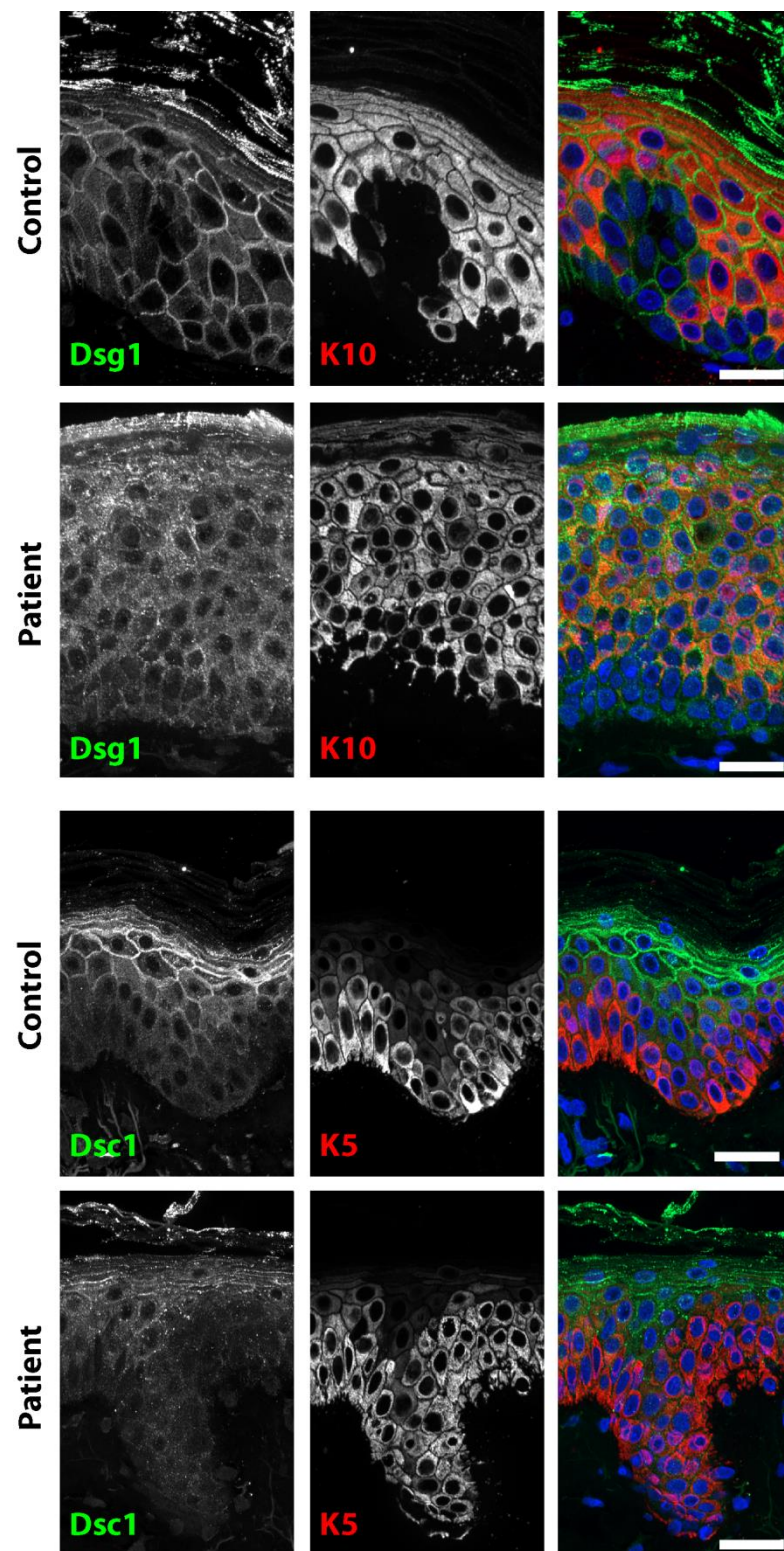


Figure S6. Desmoglein 1 (DSG1) and desmocollin 1 (DSC1) organization in patient epidermis. DSG1 and DSC1 were co-stained with keratin 10 (K10) and

keratin 5 (K5) respectively, and exhibited a disorganized appearance with increased cytoplasmic expression in patient as compared with control tissue (scale bar = 20 μm).

Figure S7

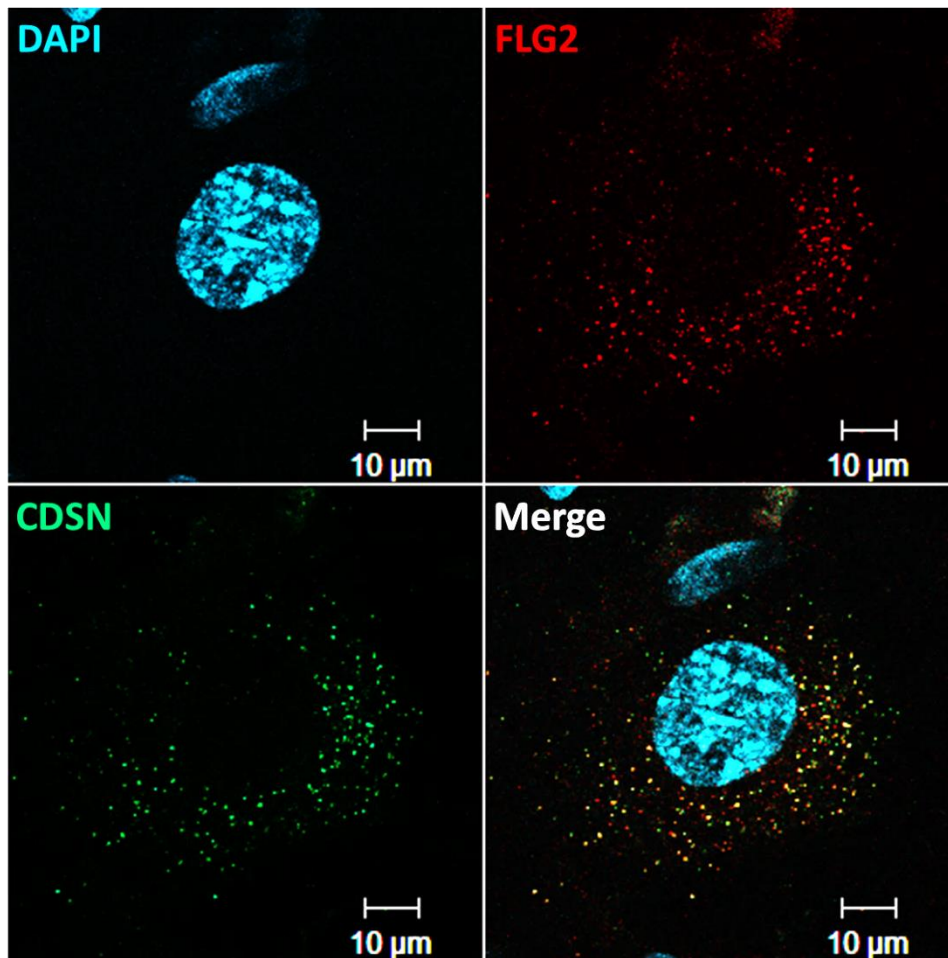


Figure S7. Filaggrin 2 (FLG2) and corneodesmosin (CDSN) expression in the keratinocytes cells. Filaggrin 2 and corneodesmosin partially co-localize by confocal microscopy (merged) in keratinocyte cells (scale bar = 10 μm).

Figure S8

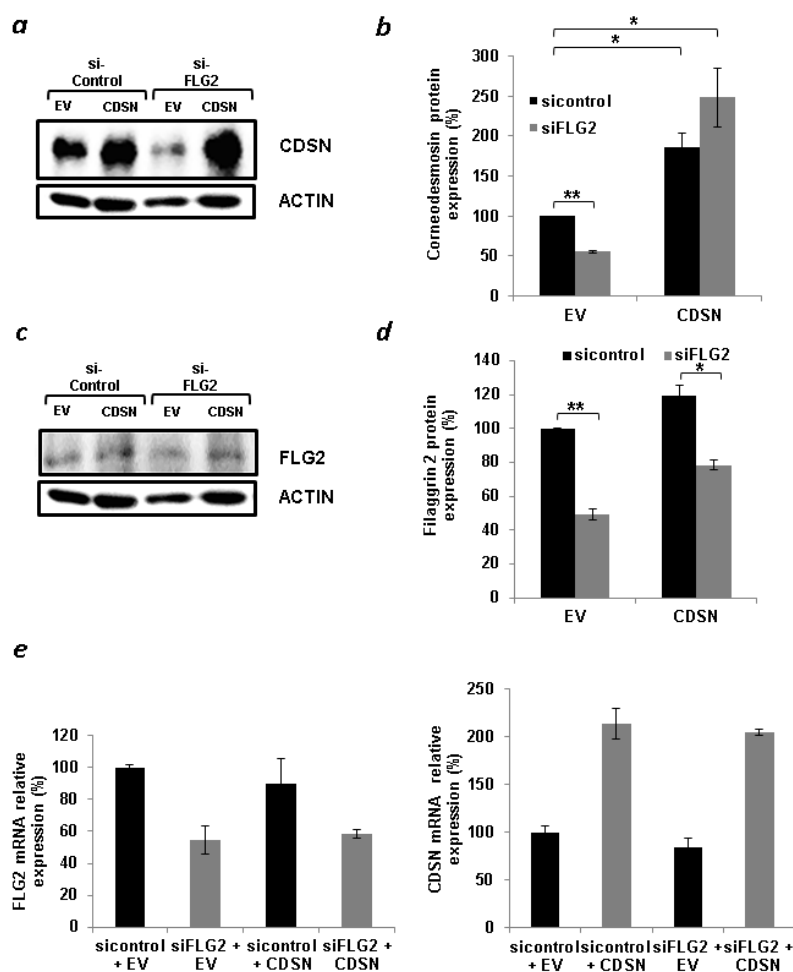


Figure S8. FLG2 and CDSN mRNA and protein expression in human epidermal keratinocyte monolayer cultures used for the dissociation assays. (a-b)

Corneodesmosin (a,b) or filaggrin2 (c,d) protein expression in human primary keratinocytes transfected with control siRNA or *FLG2*-specific siRNA together with either an empty vector (EV) or a *CDSN* (*CDSN*) expression vector was ascertained using immunoblotting with anti corneodesmosin or anti filaggrin 2 antibodies. β -actin served as a loading control; (b,d) Protein levels were quantified using ImageJ software and normalized to levels observed in siControl and EV transfected keratinocytes; (e) *CDSN* and *FLG2* mRNA levels were quantified using qRT-PCR (analysis was performed in parallel with the Western blot experiments). Results were

normalized to *GAPDH*. Results are expressed as percentage of RNA expression relative to expression in control samples \pm SEM. Results represent the mean of at least three independent experiments (two sided t-test; *p<0.05, **p<0.01).

Figure S9

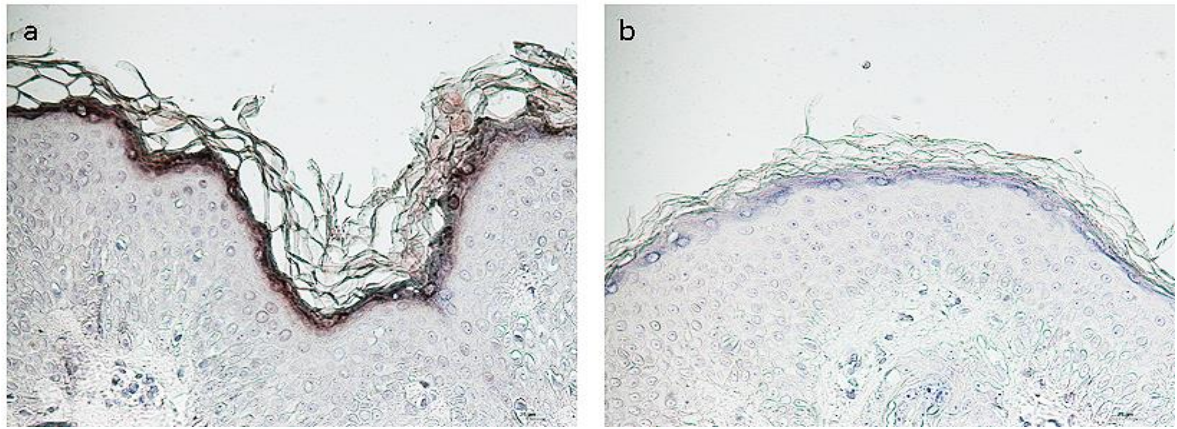


Figure S9. Immunohistochemical staining with anti-filaggrin 2 antibody. A skin biopsy was stained as described in Materials and Methods using a filaggrin-2 specific antibody which was pre-incubated with either (a) bovine serum albumin 2% or (b) or a filaggrin 2 recombinant protein antigen.

Figure S10

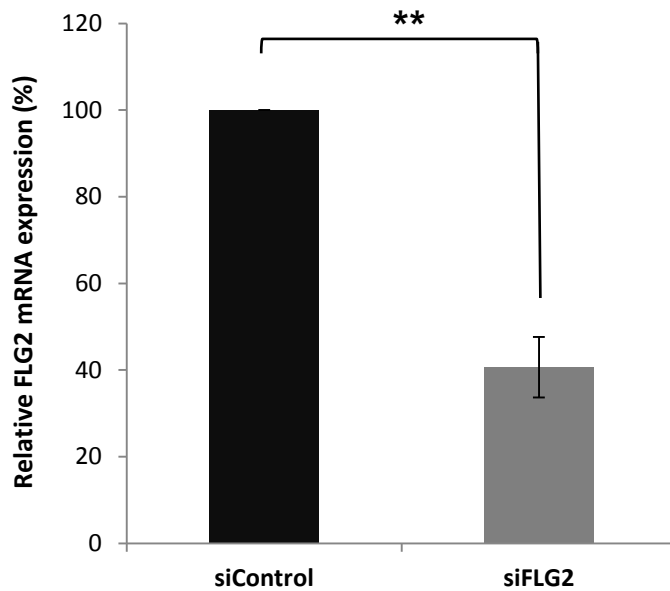


Figure S10. *FLG2* expression in human epidermal keratinocyte monolayer cultures used for dissociation assays. *FLG2* mRNA levels were quantified using qRT-PCR in epidermal monolayers treated with *FLG2*-specific siRNA- and control siRNA. Analysis was performed in parallel with the dissociation assay from the same population of keratinocytes. Results were normalized to *GAPDH*. ** $p < 0.01$, unpaired-t test.

Figure S11

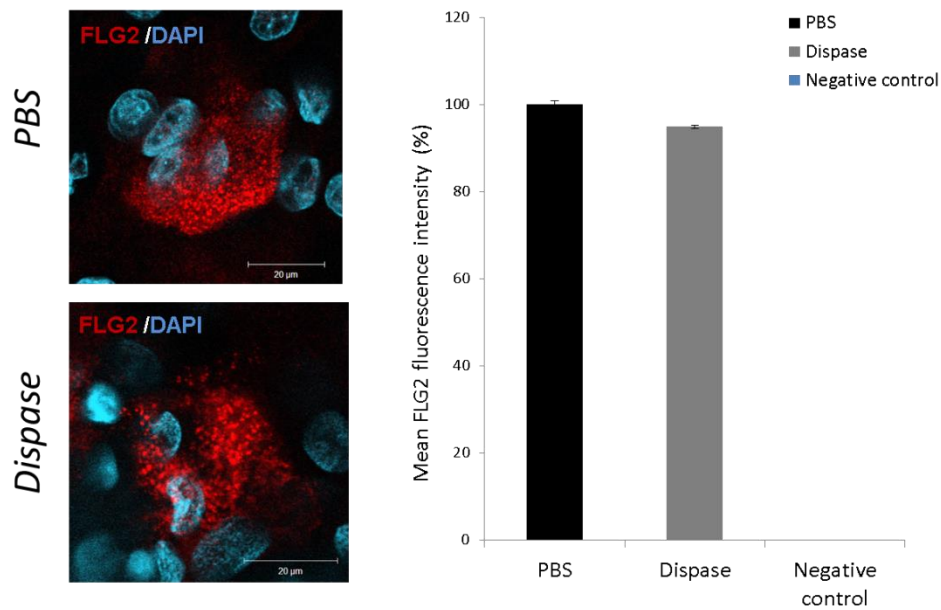


Figure S11. The effect of dispase treatment on filaggrin 2 expression.

Keratinocytes were treated with dispase or with PBS as a control according to the dispase dissociation assay protocol (see in Material & Methods section), fixed and stained with an anti-filaggrin 2 antibody. Fluorescence signal was quantified using the NIS-Elements BR 3.6 software. Seven measurements were performed per field for each fluorescence staining and normalized to the field area. Results are expressed as mean fluorescence signal \pm SEM.

SUPPLEMENTARY REFERENCES

- Adzhubei IA, Schmidt S, Peshkin L, Ramensky VE, Gerasimova A, Bork P, et al. A method and server for predicting damaging missense mutations. *Nat Methods* 2010;7:248-9.
- Fuchs-Telem D, Stewart H, Rapaport D, Noursbeck J, Gat A, Gini M, et al. CEDNIK syndrome results from loss-of-function mutations in SNAP29. *Br J Dermatol* 2011;164:610-6.
- Kumar P, Henikoff S, Ng PC. Predicting the effects of coding non-synonymous variants on protein function using the SIFT algorithm. *Nat Protoc* 2009;4:1073-81.
- Li H, Durbin R. Fast and accurate long-read alignment with Burrows-Wheeler transform. *Bioinformatics* 2010;26:589-95.
- McKenna A, Hanna M, Banks E, Sivachenko A, Cibulskis K, Kernytsky A, et al. The Genome Analysis Toolkit: a MapReduce framework for analyzing next-generation DNA sequencing data. *Genome Res* 2010;20:1297-303.
- Mildner M, Ballaun C, Stichenwirth M, Bauer R, Gmeiner R, Buchberger M, et al. Gene silencing in a human organotypic skin model. *Biochem Biophys Res Commun* 2006;348:76-82.
- Wang K, Li M, Hakonarson H. ANNOVAR: functional annotation of genetic variants from high-throughput sequencing data. *Nucleic Acids Res* 2010;38:e164.